Study of solar still in groundwater treatment in Brazilian northeast

Karyna Steffane da Silva[a], Yohanna Jamilla Vilar de Brito[a], Camylla Barbosa Silva[a], Geralda Gilvania Cavalcante de Lima[a], Keila Machado de Medeiros[b,*], Carlos Antônio Pereira de Lima[a]

[a]*Sanitary and Environmental Engineering Department, State University of Paraiba, Av. Baraúnas, 351, 58429-500, Campina Grande, Paraiba, Brazil, Tel.: +55 83 3315 3333; emails: karynasteffane@hotmail.com (K.S. da Silva), yohannajvb@gmail.com (Y.J.V. de Brito), camyllabsilva@hotmail.com (C.B. Silva), gilvania@uepb.edu.br (G.G.C. de Lima), caplima@servidor.uepb.edu.br (C.A.P. de Lima)*
[b]*Science and Technology Center in Energy and Sustainability, Federal University of Recôncavo da Bahia, Av. Centenário, 697, Sim, 44042-280, Feira de Santana, Bahia, Brazil, Tel.: +55 75 3622 9351; email: keilamedeiros@ufrb.edu.br (K.M. de Medeiros)*

Received 16 November 2022; Accepted 3 April 2023

ABSTRACT

To combat water scarcity, technologies have been developed to assist the population. Among these we can mention the desalination of brackish water by solar energy since this energy is abundant in Brazil Northeast region. Thus, two models of solar stills were built one with a double slope solar still and the other with a pyramid solar still, both with equal areas, in order to verify the potential of these stills in relation to productivity. The experiments were carried out in the city of Campina Grande/Paraiba/Brazil, being submitted to the same climatic conditions on the same day. The pyramid solar still produced an average of 2,508.0 mL·m^{-2} and the double slope solar still 2,329.0 mL·m^{-2}, which indicates a slightly higher yield of the pyramid solar still with a measure of 7.13%. This manuscript aims to contribute to the scarcity of comparative studies between stills with different formats, verifying that this greater productivity of pyramidal stills can be attributed to the fact that they receive extra sunlight because they have four sides, in addition to having a larger condensation area, obtaining water treated with potability standards for human consumption, meeting the demand for fresh water in isolated communities in semiarid regions.

Keywords: Desalination; Solar energy; Efficiency; Double slope solar still; Pyramid solar still

1. Introduction

When it comes to drinking water, we often associate this item with its scarcity, especially in places with drier climates, due to the few periods of pluviometric precipitation. An example of these places is semi-arid regions of the world, which have a great potential for solar energy and have more favorable levels of radiation when compared to other regions.

Significant increases in water and energy demands are expected due to the estimated increase in global population to 9.7 billion until 2050. On the other hand, the total amount of water available on the planet remains approximately constant, around 1.4 billion km^3, with less than 1% of fresh water for human consumption. Furthermore, accessible sweet water resources are also negatively impacted by anthropogenic actions, as well as damage caused by extreme weather events, potentially aggravated by global climate change. It is estimated that vulnerable populations due to increased water stress can reach up to 2 billion people until 2040 [1].

Arid and semi-arid areas comprise about 36% of Earth's land surface. In Brazil, 87.8% of the Northeast region is located in a semi-arid area, requiring special attention in relation to water supply, in contrast to other regions of the

* Corresponding author.

country. The Brazilian semi-arid region generally presents a more critical and prolonged dry period, in addition to its natural characteristics such as high temperatures, low thermal amplitudes, strong insolation, high rates of evapo-transpiration, and finally, low rates of rain, which leads to the low availability of water from rivers [2].

Much of the Brazilian semi-arid region has its rainy periods considerably smaller and irregular, consequently increasing the days when there are high levels of solar radiation incidence, increasing the temperatures, and turning the weather dry. The average annual precipitation ranges from 1,800 mm on east coast to 400 mm in the center of the semiarid region; while the air temperature varies 16.8°C to 33.8°C and the evaporation can exceed 10 mm·d^{-1} [3].

Salinity is a common characteristic in soils and subsoils of Brazil's semi-arid regions, due to great predominance of crystalline rocks. Many soils are shallow, rocky, with low porosity values, and with low permeability, slow circulation of fluids and, consequently, a longer contact time between the water and the crystalline body (rich in salts), thus causing greater salinization of local waters, which directly affects the waters of wells drilled in this region [4].

In a remote area where there is a shortage of drinking water, but with an abundant amount of solar radiation. Therefore, solar desalination is the most suitable form of energy that can be used to provide cheap drinking water using decentralized methods. This is a fundamental solution because most remote and rural areas, especially those in arid regions, have abundant sources of solar radiation that can be used as power supply to produce drinking water [5,6]. Desalination by solar energy is an old technique, but it has been widespread in places propitious to its use.

These devices generally imitate a part of the natural hydrological cycle, in which saline water is heated by the sunlight to promote the production of water vapor. The water vapor is then condensed on a cold surface and collected as fresh water [7]. Solar distillation is seen as an effective alternative of clean technology, as it entails minimal damage to the environment, taking advantage of the abundant and free energy sources found in these regions. Over time, several models of stills have been created in order to obtain greater productivity of desalinated water. Currently, several authors have dedicated themselves to the study of the process of desalination of brackish waters by solar energy, with several different models of stills [8].

Desalination systems using solar energy can be classified in several ways. According to the method by which the thermal energy is received in active or passive form. They can still be classified as high or low temperature. The Fig. 1 shows the different ways that these classifications can happen, and which researcher worked with each system [9–25].

The various factors that affect the productivity of a solar still are solar radiation intensity, wind speed, ambient temperature, water-glass temperature difference, free water surface area, absorber plate area, inlet water temperature, glass angle and depth of water slide. These parameters are subject to change [26,27]. Solar intensity, wind speed, ambient temperature, are metrological parameters and are not controllable by man [28].

In this sense, many studies have been carried out in order to verify the influence of these parameters on the performance of solar stills. Several researchers investigated the depth of the water in the desalination basin. All of them agreed that the depth of water is considered the parameter that most affects the performance of the still and that it is inversely proportional to its productivity [29–31].

The thermal storage of latent heat from condensation vapor of the solar stills by phase change materials (PCMs) is also a subject of investigations. Faegh and Shafii [32] noted that the yield increases 86% when compared to the yield of the system without PCM, reaching 6,555 kg·m^{-2}·d^{-1} with an efficiency of 50%.

The simplest model of desalinator is the single slope solar still [34–36]. Other simple operation models have also been extensively studied, such as the double-slope solar still [37–39] and the pyramidal solar still [40–42]. It is noteworthy that the basic mechanism of drinking water production is similar between these two models. Several changes were introduced to improve the efficiency of these desalinators for the double slope [43,44] and for the pyramidal [45,46]. Furthermore, there are few comparative studies regarding
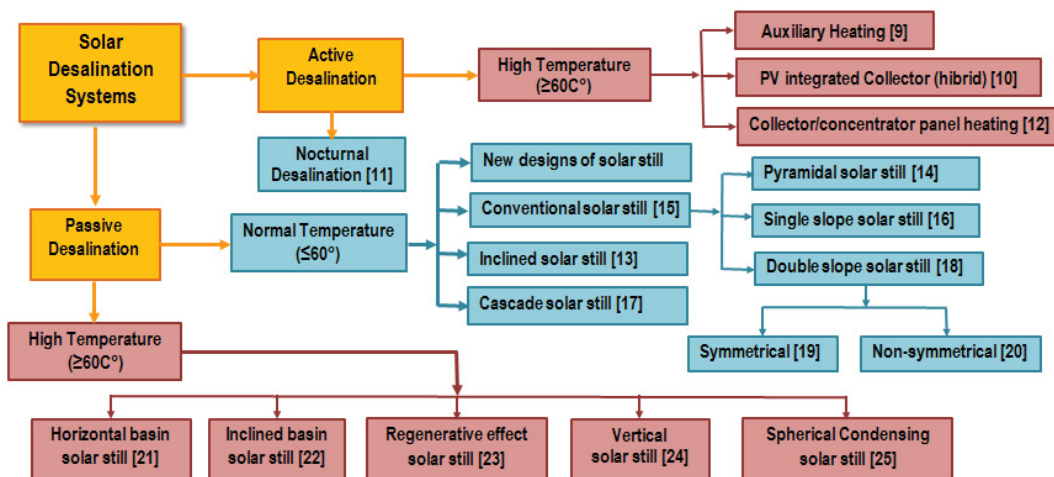
Fig. 1. Classification of solar distillation systems.

their them. In addition to these simpler configurations, several materials, arrangements or models of solar stills are produced and improved in order to increase efficiency in water production, materials that store thermal energy can be added to them [47–49], can be performed modification in their structures [50,51] or as a combination of materials and new desalination models [52–57] that aim to improve the desalination process by increasing the heat absorption area, the condensation area, as well as the thermal energy storage.

Solar desalination has become a suitable solution to overcome the scarcity of fresh water in isolated regions, being a source of renewable energy. Small-scale desalination systems represent a valuable source of freshwater supply when salt or brackish water is available. Therefore, this fact demonstrates the importance of developing solar desalinators as a viable alternative, using low-cost materials, easy to acquire and that meet the desired characteristics, for good functionality and efficiency in obtaining treated water with potability standards for consumption in order to meet the demand for fresh water in isolated communities. This research aims to contribute to the scarcity of specific studies by carrying out a comparative analysis between passive stills with the same area of sun exposure, but with different formats, in order to verify whether this characteristic influences the temperature profiles and the productivity of desalinated water, selecting the most efficient for application in semiarid regions of Brazilian northeast.

2. Experimental set-up

2.1. Experiments location

The experiments were carried out in the city of Campina Grande – Paraiba/Brazil, at latitude 7°13′11″ south and longitude 35°52′31″ west, with an average altitude of 550 m above sea level, at the Research Laboratory in Environmental Sciences, from the Department of Sanitary and Environmental Engineering of the Science and Technology Center of the State University of Paraiba. The stills were fed with brackish water collected from a well in the city of Juazeirinho – Paraiba/Brazil (latitude 7°4′1″ south and longitude 36°24′42″ west). This well was selected because it is a source of water supply for the local community. The cities of Campina Grande and Juazeirinho are in the semiarid zone of Brazil.

2.2. Water portability parameters

Water generally contains several components, which come from the natural environment or were introduced from human activities. To characterize water, several parameters are determined, which represent its physical, chemical and biological characteristics. These parameters are indicators of water quality and when they reach values higher than those established for a given use, this water is considered inappropriate [58]. The main indicators that demonstrate the quality of water in relation to its degree of salinity are shown in Table 1. The brackish waters were characterized before and after the desalination process by these parameters.

2.3. Measuring system

Solar radiation was measured using a KIMO SL100 pyranometer (1.0–1,300.0 W·m^{-2}) with an accuracy of ±1.0 W·m^{-2}. Temperatures at different points of the system were measured using a digital K-type thermometer with a range –50°C–300°C and accuracy of ±1.0°C. All readings are sent to the laptop by the data acquisition system. The water produced was measured using a graduated laboratory vessel (0–1,000.0 mL) with an accuracy of ±10.0 mL. Errors occurred in the measuring instruments are shown in Table 2. The errors were calculated for thermocouples, solar meter, and collecting vessel. The maximum error that occurred in any instrument is equal to the ratio between its minimum count and the minimum value of the measured output.

2.4. Solar stills description

Two passive solar stills were used, they were constructed so that they had the same area of exposure to the sun, but with different formats. They are made of 1.0 mm thick aluminum foil, internally they are painted with matte black for better absorption of solar radiation, and they are covered with 4.0 mm thick glass blades. On the internal sides there are gutters for collecting condensed water. The external sides and the base of stills are insulated using 10.0 mm thick fiberglass to prevent heat loss to the environment. The pyramid solar still has the following dimensions, 0.50 m in length, 0.50 m in width and 0.10 m in height, presenting a useful area for desalination of 0.25 m². The double slope solar still is 1.25 m long, 0.20 m wide and 0.10 m high, also presenting a useful area for desalination of 0.25 m², as can be seen in Fig. 2.

2.5. Solar stills operational mode

In order to verify the influence of the shape of the stills on their production, they were operated in the same place,

Table 1
Physical and chemical parameters used

Physico-chemical properties	Unity
pH	–
Electric conductivity	µS·cm^{-1}
Total hardness as CaCO$_3$	mg·L^{-1}
Total alkalinity as CaCO$_3$	mg·L^{-1}
Sodium as Na$^+$	mg·L^{-1}
Chlorides as Cl$^-$	mg·L^{-1}
Turbidity	NTU

Table 2
Accuracy and errors for measuring instruments

Instrument	Band	Accuracy	Error %
Radiometer	1 to 1,300.0 W·m^{-2}	±10 W·m^{-2}	5.0%
Digital thermometer	–50°C to 300°C	±0.1°C	0.25%
Graduated cylinder	0 to 1,000.0 mL	±10 mL	1.0%
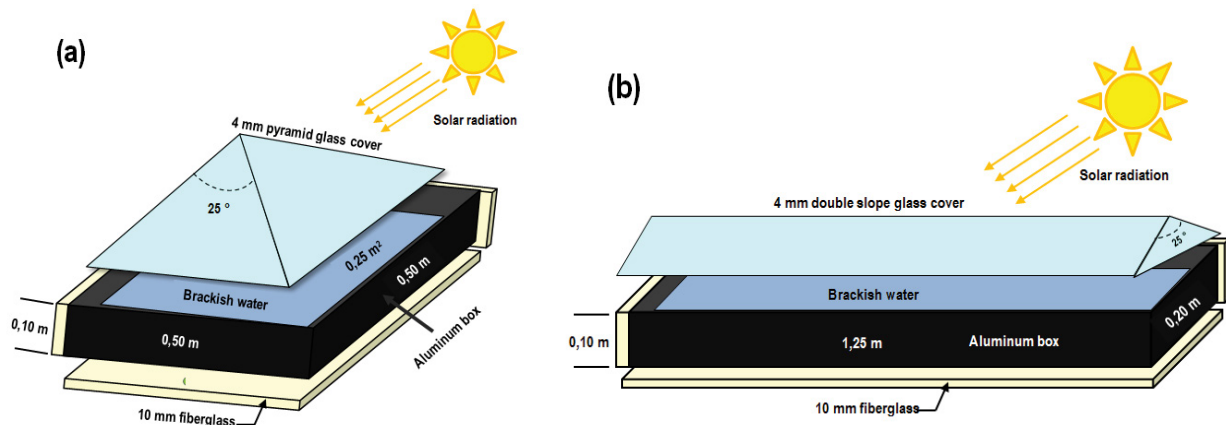
Fig. 2. Stills description: (a) pyramid solar still and (b) double slope solar still.

at the same time and in the same environmental conditions. They were fed with brackish water collected in the well of Juazeirinho city located in the state of Paraiba. The operation of the equipment was carried out in batches, and a thickness of 1.0 cm brackish water was defined for both stills.

Temperature measurements were made at various points of the stills (water, glass, and in the basin), in addition to measurements of the ambient temperature. Every temperature measurement was make using thermocouples of type PT-100 made of metal alloys. The radiation measurement was performed using the SL 200 17957 radiometer of the KIMO brand, and the amount of distillate was measured using a graduated cylinder. Details are shown in Fig. 3.

The experiments took place in the months of November and December 2021, from 7:00 am to 5:00 pm. Four experiments were performed on the 26th, 27th, 28th of November and another one on the 2nd of December 2021.

The measurements of the variables happened continuously, every 30 min, the value of the desalinated water obtained was recorded. At the end of the day for each experiment, the total volume of desalinated water reached was recorded.

3. Thermal model

There are certain difficulties in modeling a solar desalination system because of the transient and variable characteristics as well as the fact that the intensity of solar radiation is not homogeneous from region to region.

The model that presents productivity and efficiency in a certain country, as in Brazil, may not occur in other countries. Theoretical calculations for determining the performance of the solar desalinator will depend on the use of empirical heat exchange coefficients. The main models existing in the literature are based on the relationships presented by Dunkle [15].

For the execution of the mathematical modeling, the following hypotheses were accepted as a basis:

- The temperature of each component is uniform;
- At the beginning of the process, the temperatures on all surfaces are equal to the ambient temperature;
- Condensation occurs only on the glass cover;
- The desalinator is free of leaks;
- The desalinator operates in a transient regime.

3.1. Heat transfer modes in solar stills

The heat transfer processes in a solar desalination system can be classified into internal and external processes based on the flow of energy inside and outside of the enclosed space. The internal heat transfer is responsible for the transport of pure water in the form of steam leaving behind the basin's impurities, while the external heat transfer through the condensation cover is responsible for the condensation of the pure steam as distillate [59]. The numerical results are obtained by solving the energy balance equations for the glass cover, brackish water slide, basin, and solar desalination isolators, as shown in Fig. 4.

Initially, the thermal balance in the condensation glass was made. The water condensation occurs in this part of the equipment, which after evaporating goes to the glass, because it has a lower temperature, thus occurring the condensation of the distillate.

The energy variation in the condensing glass is calculated by the difference between the energy that is reaching the glass cover and the energy that is leaving. Irradiation, evaporation, radiation and water convection are reaching the glass cover. The radiation and the convection are leaving the glass, as expressed in Eq. (1). In the subsequent equations, T_a, T_{sky}, T_g, T_w, T_b and T_{ins} are average ambient temperature, sky temperature, glass cover temperature, brackish water temperature, basin temperature and insulator temperature, respectively, all measured in °C.

$$m_g \cdot C_g \cdot \frac{dT_g}{dt} = \alpha_g \cdot I(t) \cdot A_g + h_{ewg} \cdot A_g \cdot \left(T_w - T_{gi}\right)$$
$$+ h_{cwg} \cdot A_g \cdot \left(T_w - T_{gi}\right) + h_{rwg} \cdot A_g \cdot \left(T_w - T_{gi}\right)$$
$$- \left[h_{cga} \cdot A_g \cdot \left(T_{ge} - T_a\right) + h_{rgs} \cdot A_g \cdot \left(T_{ge} - T_{sky}\right) \right] \quad (1)$$

In the thermal balance for the water, the energy that is reaching the brackish water is the irradiation that passes
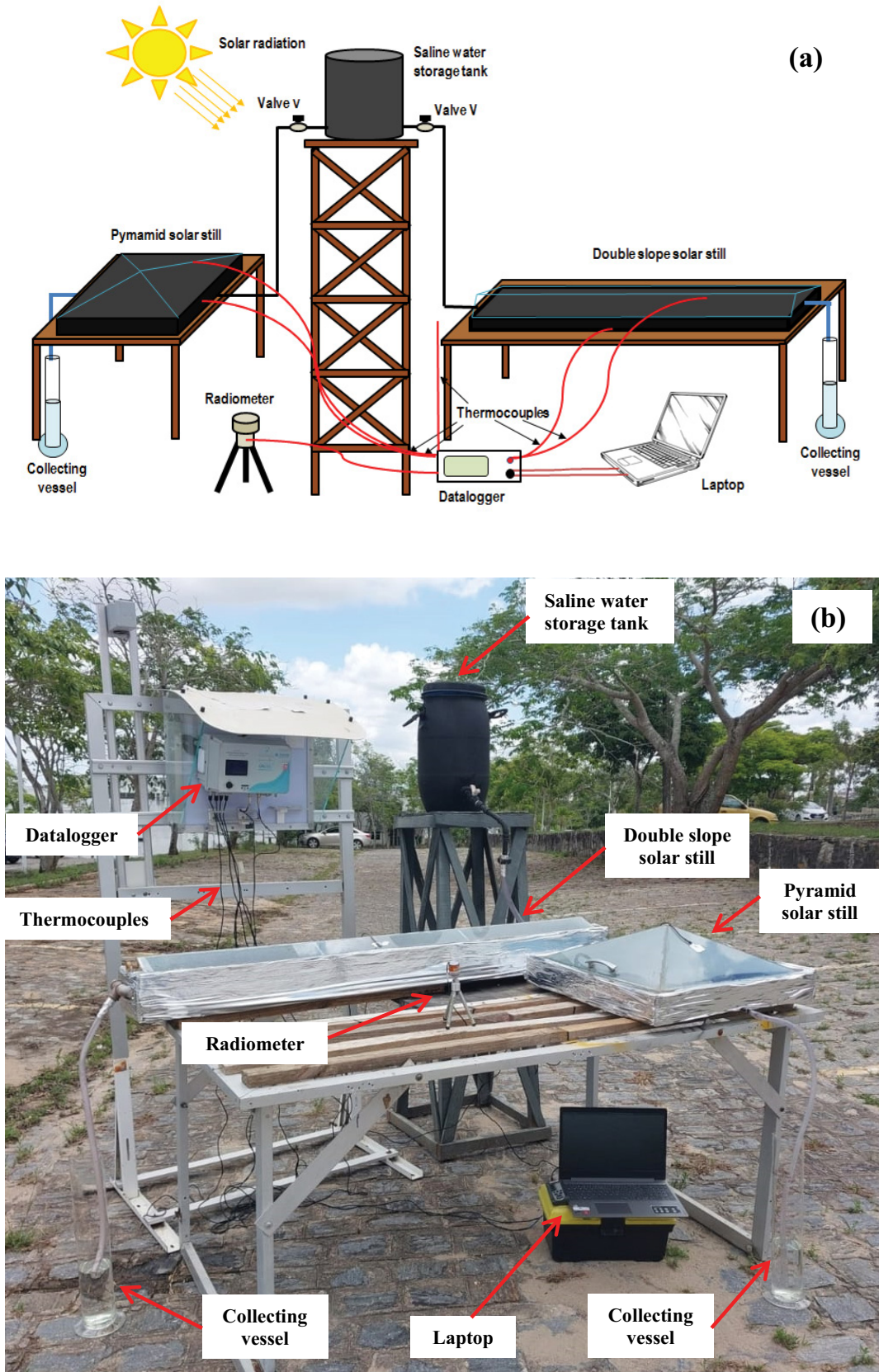
Fig. 3. Experimental desalination system, (a) schematic diagram and (b) photographic view of system experimental.
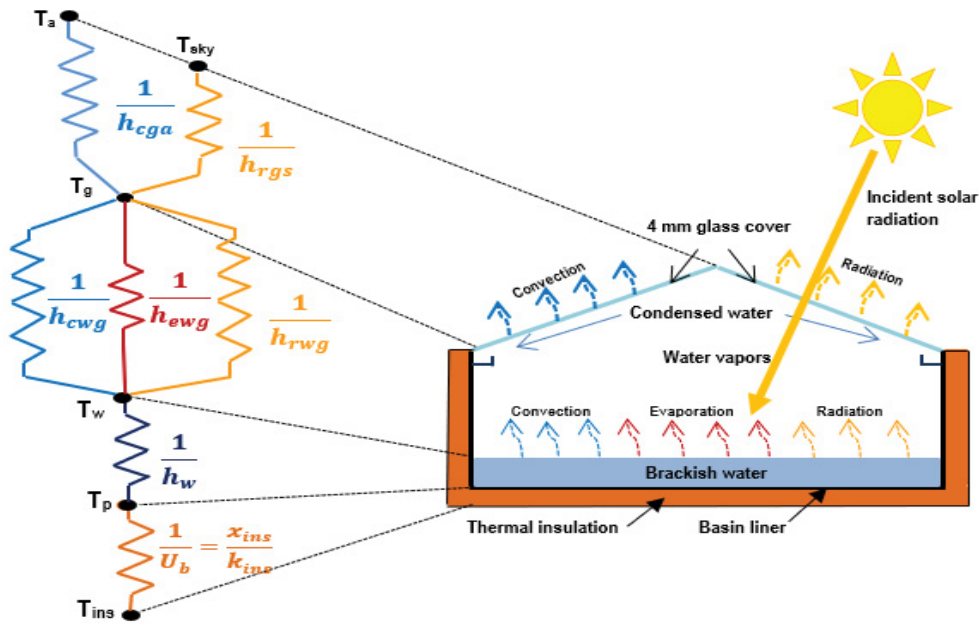
Fig. 4. A schematic diagram of the double slope solar still and pyramid solar still and the thermal resistance networks of the still elements.

through the glass cover until it reaches the water and the conduction that occurs between the water and the basin. The energy that comes out is convection, radiation and evaporation that occurs between the water and the glass. The difference between the energy that arrives and that leaves the brackish water is the variation in energy that occurs in this system, as represented in Eq. (2):

$$
m_w \cdot C_w \cdot \frac{dT_w}{dt} = \left[\tau_g \cdot \alpha_w \cdot I(t) \cdot A_w + \frac{K_w}{L_w} \cdot A_w \cdot (T_b - T_w) \right]
$$
$$
- \left[\begin{array}{c} h_{ewg} \cdot A_g \cdot (T_w - T_{gi}) + h_{cwg} \cdot A_g \cdot (T_w - T_{gi}) \\ + h_{rwg} \cdot A_g \cdot (T_w - T_{gi}) \end{array} \right] \quad (2)
$$

The basin is the place where the water is stored for that entire desalination process. The energy variation is calculated by the difference between the energy that is arriving and the energy that is leaving the basin. The irradiation, which passes through the glass and the water, and the conduction that occurs with the water are reaching the basin. The conduction between the basin and the insulator is leaving the system, as expressed in Eq. (3).

$$
m_b \cdot C_b \cdot \frac{dT_b}{dt} = \tau_g \cdot \tau_w \cdot \alpha_b I(t) \cdot A_b + \frac{K_b}{L_b} \cdot A_b \cdot (T_b - T_w)
$$
$$
- \left[\frac{K_{ins}}{x_{ins}} \cdot A_{ins} \cdot (T_b - T_{ins}) \right] \quad (3)
$$

3.2. Internal heat transfer coefficients

The heat exchange between the water surface and the inner surface of the glass cover is known as internal heat transfer. There are three heat exchange types, convection, radiation and evaporation processes, by which the internal heat transfer process within the system is governed.

According to Aggarwal and Tiwari [60], the convective coefficient of heat exchange between brackish water and the glass cover (h_{cwg}) can be calculated as in Eq. (4):

$$
h_{cwg} = 0.884 \left[(T_w - T_{gi}) + \frac{(P_w - P_g)(T_w + 273.15)}{268.9 \times 10^3 - P_w} \right]^{\frac{1}{3}} \quad (4)
$$

The h_{rwg}, radiative heat exchange coefficient between brackish water and the glass cover, can be expressed in Eq. (5), proposed by Abu-Arabi et al. [61]:

$$
h_{rwg} = \frac{\sigma (T_w^2 + T_g^2)(T_w + T_g)}{\frac{1}{\varepsilon_w} + \frac{1}{\varepsilon_g} - 1} \quad (5)
$$

Zurigat and Abu-Arabi [62] describe that the evaporative heat exchange coefficient between brackish water and the glass cover h_{ewg}, which can be defined in Eq. (6):

$$
h_{ewg} = 16.273 \times 10^{-3} \times h_{cwg} \times \frac{(P_w - P_g)}{(T_w - T_g)} \quad (6)
$$

where P_w and P_g are the water vapor pressures in brackish water and glass cover, respectively. they are calculated as suggested by [63] in the Eqs. (7) and (8):

$$
P_w = \exp\left(25.317 - \frac{5144}{T_w + 273.15} \right) \quad (7)
$$

$$P_g = \exp\left(25.317 - \frac{5144}{T_g + 273.15}\right) \tag{8}$$

3.3. External heat transfer coefficients

External heat transfer consists of conduction, convection and radiation processes. Thermal energy that leaves the solar still into the atmosphere is considered loss. The heat lost in the solar still from the outer surface of the glass cover to the atmosphere is called superior heat loss transfer process, and that of the brackish water to the atmosphere through insulation is called heat loss transfer process of the bottom and of the side.

According to Madhuri and Tiwari [64], the external heat transfer coefficients in the desalinator can be calculated by:

The convective coefficient of heat exchange between the glass cover and the ambient air is calculated according to Eq. (9).

$$h_{cga} = 2.8 + (3.0 \times v) \tag{9}$$

v is used to express the wind speed.

The radiative heat transfer coefficient between the outer surface of the glass cover and the environment is calculated by Eq. (10).

$$h_{rgs} = \varepsilon_g \sigma \left[\frac{\left(T_g + 273\right)^4 - \left(T_{sky} + 273\right)^4}{\left(T_g - T_a\right)} \right] \tag{10}$$

4. Results and discussions

In order to evaluate the influence of the shape of the stills on productivity of desalinated water some parameters were analyzed, such as the incidence of solar radiation, the ambient temperature, the water temperature and the glass cover temperature. All these parameters will lead to a greater or lesser productivity of desalinated water in each still type. The two stills were subjected to the same climatic conditions, positions and orientations. It is important to point out that the transient operational conditions that govern the processes with solar energy will result in fluctuations in the results related to solar radiation over time, influencing the variations of the parameters, among them: temperature profile, instantaneous water production, efficiency of the desalinators, as well as the heat transfer coefficients presented in the results below.

4.1. Intensity of solar radiation

The intensity of solar radiation has an important effect on performance of solar stills [65]. The variations in temperature of the glass cover, the water temperature, and the ambient temperature as a function of the incident radiation for the pyramid type still and double slope still, for the 1.0 cm water depth were studied on November 26th, 2021. The temperature and radiation profiles are shown in Fig. 5. The intensity of solar radiation was measured at the location of the experiments. The variation of solar intensity of

the experiment for the pyramid still, has a distribution that follows the climatic conditions at the time of measurement. The maximum radiation is received is around 11:30 am with a value of 1,301.0 W·m^{-2}, as you can see in the solar radiation intensity curve.

According to Fig. 5, throughout the experiment, the temperature of the brackish water changes, starting at 07:00 am with 26.0°C and reaching the highest value of 77°C at 12:30 pm, an hour after the moment of greatest incidence of solar radiation. Similar behavior was obtained with the double slope still, with maximum temperature of 73°C obtained at 12:30 pm, half an hour after the moment of greatest incidence of solar radiation, indicating that the temperature of the pyramid solar still was 5.19% higher than the double slope solar still. Also, according to Fig. 5, throughout the experiment, the temperature of the brackish water changes, starting at 07:00 am with 26.0°C and reaching the highest value of 75°C at 12:00 pm, half an hour after the moment of greatest incidence of solar radiation. Similar behavior was verified by Kumar et al. [66] where they obtained temperature variations for the pyramid solar still with a maximum temperature of 61°C for the tray and 41°C for the glass cover, while Al-Molhem and Eltawil [67] studying a double slope solar still obtained a maximum temperature of 62.8°C for the tray and 56°C for the glass cover.

4.2. Desalinated water production

The weather plays a vital role in the use of solar energy. The production of the system is directly related to the energy that comes from the sun. There is a direct correlation between the intensity of solar radiation and the amount of desalinated water produced: higher solar radiation provides a greater production of desalinated water. Productivity is directly proportional to solar radiation at constant temperature, in kJ·m^{-2} [68]. Four experiments were carried out on November 26th, 27th, 28th and December 2nd, 2021.

4.2.1. Instant desalinated water production

Fig. 6 shows the instantaneous production of desalinated water from the pyramid still and double slope still on
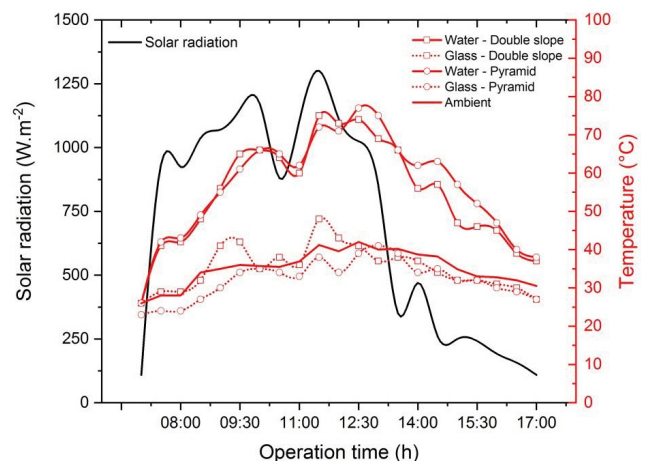
Fig. 5. Temperature profiles as a function of solar radiation.

11/26/2021 with an average solar radiation of 699.85 W·m^{-2}·d^{-1}. In the morning, the radiation gradually increased with maximum peak occurring at 11:30 am. For the pyramid still, the maximum production of 375 mL·h^{-1}·m^{-2} occurred at 12:00 pm, this time difference with respect to radiation is due to delay in the system response time [69]. The double slope still had a similar behavior, the maximum production of 336 mL·h^{-1}·m^{-2} occurred at 12:30 pm. The peak of instantaneous water production of the 176 mL double slope solar still observed at 2:30 pm and 99 mL at 4:00 pm for the pyramid solar still is due to the accumulation of water in the condensate collection trough, which sometimes does not drain completely and when the flow occurs to the test tube, all the accumulation is retained in the trough. For both cases, it is interesting to note that production of desalinated water has the same profile as solar radiation. Al-Hinai et al. [70] when studying a double slope still obtained the same behavior for water productivity in relation to solar radiation.

4.2.2. Accumulated production of desalinated water

The evolution of accumulated desalinated water production, for the pyramid solar still and for the double slope solar still, are shown in Fig. 7 on 11/26/2021. The accumulated water production per area of desalination unit is registered at 17:00 pm and is 2,376.0 mL·m^{-2}, for the pyramid still. At the beginning of the experiment, the desalination system is in stationary state with the temperature at 26°C, as time passes the water heats up and at 12:30 pm it reaches a maximum temperature of 77°C for the desalinator. The evolution of accumulated desalinated water production by area of desalination unit, for the double slope solar still, is recorded at 17:00 pm and is 2,320.0 mL·m^{-2}. Initially the desalination system is in a with temperature at 26°C, over time the water heats up and at 11:30 am it reaches a temperature of 75°C. From 8:30 am the production of desalinated water begins, which increases with the increasing temperature and continues its production until 17:00 pm. Desalinized water accumulation curves in desalinators have characteristic shapes with an ever-increasing trend, as can be seen in the research of Aburideh et al. [71] Gnanaraj and Gnanaraj [72].

Table 3 shows the production of desalinated water for the two types of solar stills studied. For November 26th, 2021, a total of 2,376.0 mL·m^{-2}·d^{-1} was obtained in the pyramid still and 2,320.0 mL·m^{-2}·d^{-1} for the double slope still. For November 27th, 2021, the pyramid solar still ended with a volume of 2,080.0 mL·m^{-2}·d^{-1} and the double slope solar still with the volume of 1,780.0 mL·m^{-2}·d^{-1}. The third day of the experiment was carried out on November 28th, 2021, with the total volume of 2,800.0 mL·m^{-2}·d^{-1} for the pyramid solar still and 2,640.0 mL·m^{-2}·d^{-1} for the double slope solar still.
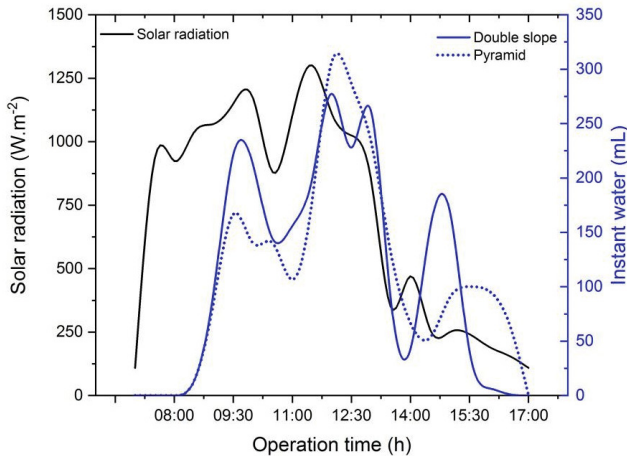
Fig. 6. Instant water production from the pyramid solar still and double slope solar still.
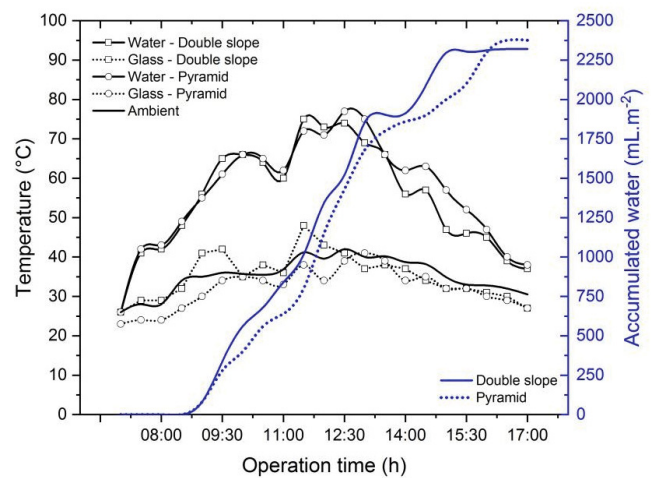
Fig. 7. Water production in the pyramid solar still and in the double slope solar still.

Table 3
Volume produced and the stills efficiency

Dates	Average radiation (W·m^{-2})	Production (mL·m^{-2}·d^{-1})		Daily efficiency (%)	
		Pyramid solar still	Double slope solar still	Pyramid solar still	Double slope solar still
11/26/2020	699.85	2,376.0	2,320.0	12.65	10.92
11/27/2020	592.47	2,080.0	1,780.0	7.09	5.16
11/28/2020	761.09	2,800.0	2,640.0	10.42	9.89
12/02/2020	802.61	2,776.0	2,576.0	20.29	19.81
Average	714.01	2,508.0	2,329.0	12.61	11.44

The December experiment took place on the 2nd, on this day the pyramid still reached a volume of 2,776.0 mL·m^{-2}·d^{-1} and the double slope solar still of 2,576.0 mL·m^{-2}·d^{-1}. Therefore, in general, the pyramid solar still had slightly higher production of distillate volume than the double slope still, with percentages of (2.35%, 14.4%, 5.7% and 7.2%). For the experiments carried out, this higher productivity can be attributed to the fact that it receives extra solar rays due to its four sides, which allows more solar radiation to be trapped inside the desalinator throughout the day [73].

5. Efficiency of solar stills

The efficiency of a solar still with respect to the absorbed solar energy can be of two types: hourly efficiency and daily efficiency. Hourly efficiency reflects the relationship between the average latent heat generated by the water produced hourly and the total amount of solar energy absorbed. The variation in solar irradiance during the day obviously generates an hourly variation of the efficiency of the solar energy [74]. The hourly efficiency was calculated using Eq. (11) [75]:

$$\eta_h = \frac{\left(M_w \times \lambda_w\right)/3600}{\left(A_b \times I\right)} \tag{11}$$

And the latent heat of water vaporization was calculated according to Eq. (12) [76]:

$$\lambda_w = \begin{pmatrix} 2501.9 - 2.40706 T_w + 1.192217 \times 10^{-3} T_w^2 \\ -1.5863 \times 10^{-5} T_w^3 \end{pmatrix} \times 10^3 \tag{12}$$

The evolutions of the hourly efficiency for the pyramid and double slope types of stills are shown in Fig. 8 on 11/26/2021. The hourly efficiency of the stills increases with time and has the same behavior as the solar incident radiation index, however, the accumulation of condensed water in the troughs of the solar still, which, when released into the beaker, cause peaks in the calculations of their
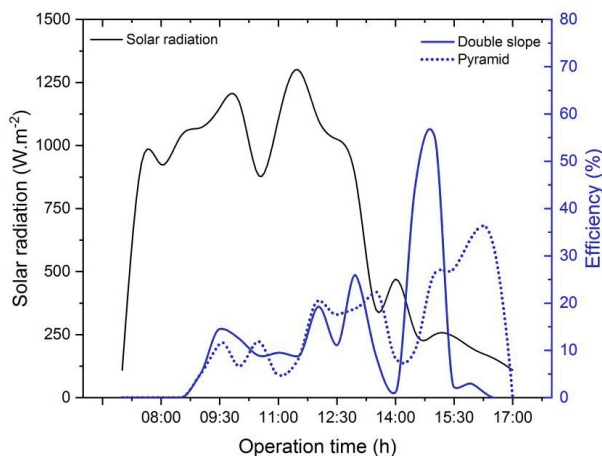
efficiencies, which justifies the greater efficiencies at the end of the day, with maximum values of 32.3% and 55.2% that were reached at 4:30 pm for the pyramid solar still and at 3:00 pm for the double slope solar still, similar behavior seen by Rahbar et al. [77].

Daily efficiency was calculated by Eq. (13) [78] and is shown in Table 3.

$$\eta_d = \frac{1}{n}\sum_n \eta_h \tag{13}$$

6. Heat transfer coefficients in solar stills

The analysis of convection, radiation and evaporation heat transfer coefficients for the two solar still is covered in this topic. Convection curves are related to the movement of the fluid, due to the increase in temperature and the displacement of the fluid horizontally or vertically. The radiation curves are directly related to the temperature of the brackish water, the glass cover and the emissivity of the glass and the water. The evaporation curves have higher values than the previous ones and they are generally more sensitive to temperature variation.

6.1. Internal heat transfer coefficients

Fig. 9 shows the curves of the internal convection, evaporation and radiation coefficients for the double slope solar still and pyramid solar still. For the double slope solar still, the evaporation coefficient reaches its peak at 11:30 am in the amount of 55.97 W·m^{-2}·K^{-1}. The curves of the convection and radiation coefficients have little variation, reaching 3.71 and 7.53 W·m^{-2}·K^{-1}. For the pyramid solar still, the curves of the convection and radiation coefficients reaches 3.94 and 7.31 W·m^{-2}·K^{-1}, respectively. The evaporation coefficient curve tracks the radiation index, and reaches its maximum value at 12:30 pm, 55.89 W·m^{-2}·K^{-1}. Al-Sulttani et al. [79] studied the heat transfer coefficients for a hybrid dual-slope solar still. they obtained an evaporation coefficient of 66.61 W·m^{-2}·K^{-1}. Results close to those found by

Fig. 8. Hourly efficiency of the pyramid still and double slope still.
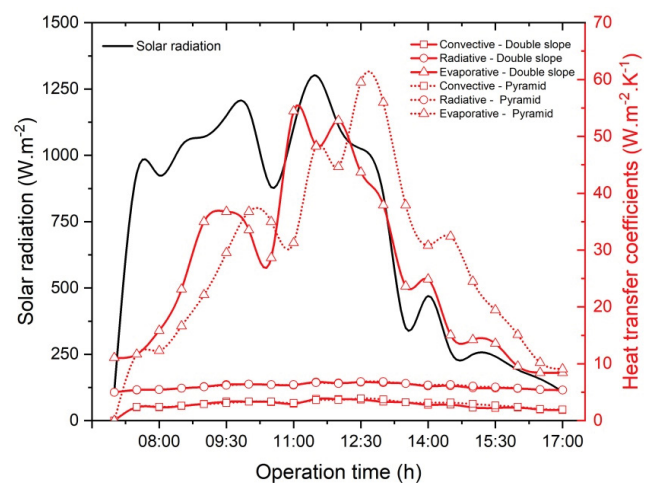
Fig. 9. Internal heat transfer coefficients.

Setoodeh et al. [80], who analyzed the heat transfer coefficients in a basin solar still and found the evaporative coefficient, using the Dunkle method, close to 30 W·m⁻²·K⁻¹.

6.2. External heat transfer coefficients

External heat transfer consists of the convection and radiation processes, which are independent of each other. The desalinator must be well insulated at the base and on the sides to reduce conduction losses. The desalinator loses heat from the outer surface of the glass cover to the atmosphere and this process is called the superior heat loss transfer process, while the heat loss from the water body to the atmosphere through insulation is called the heat loss transfer process from bottom and side. Convection curves are related to the movement of the fluid, due to the increase in temperature and the displacement of the fluid horizontally or vertically. The radiation curves are directly related to the temperature and emissivity of the glass.

Fig. 10 shows the curves of the external convection and radiation coefficients for the double slope solar still and pyramid solar still. Due to the way in which the radiation coefficients for the two solar still were calculated, they have the same value and follow the solar radiation index that hits the desalinator. The radiative coefficients are higher than the convective coefficients, obtaining the maximum values of 53.21 and 15.7 W·m⁻²·K⁻¹, respectively. The variations in the external radiation coefficients are related to the temperature differences between the external glass, the sky temperature and the ambient temperature, when the difference between the glass temperature and the ambient temperature is minimal the value of the radiation coefficient increases proportionally, as can be seen in Fig. 10. The external convection coefficients are related to the wind speed that acts on the solar still and follows the solar radiation index.

7. Thermal analysis of the solar stills

The energy balance profiles in the glass, water and basin were calculated based on the equations reported by Elango et al. [59] and described by the energy balance equations.

When performing the thermal analysis of solar still, verifying the theoretical and the experimental temperature in each component, it was possible to observe that the theoretical temperature of the glass, water and basin profiles, compared to the experimental values, were in agreement.

According to Fig. 11, the temperature profiles of the glass showed equivalent values throughout the experiment. The small difference in values that occurred was due to the direct influence of the external heat transfer coefficients. Maximum temperature values of 48°C were reached at 12:00 pm and 45°C at 13:00 pm, for the double slope solar still and pyramid solar still, respectively.

Fig. 12 shows the temperature profiles for the water. There was agreement between the experimental and theoretical values for the two solar stills. The experimental temperature values were higher than the theoretical values. The maximum temperature values were 78°C at 12:30 pm and 75°C at 12:00 pm, for the pyramid solar still and double slope solar still, respectively.

According to Fig. 13, a similarity was seen between theoretical and experimental values obtained for the absorber
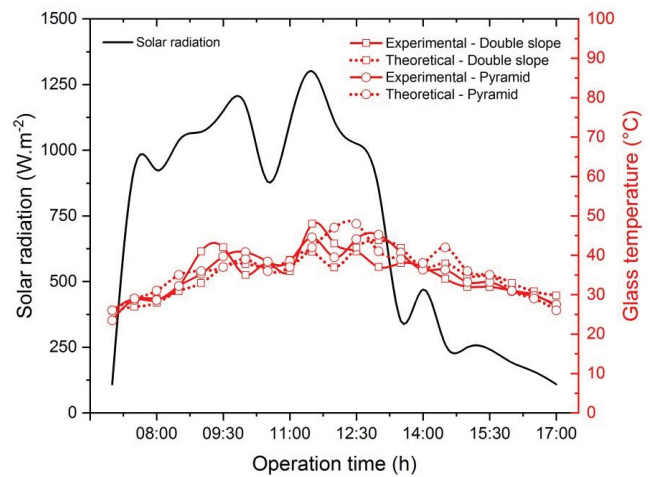
Fig. 11. Temperature profiles for the glass component.
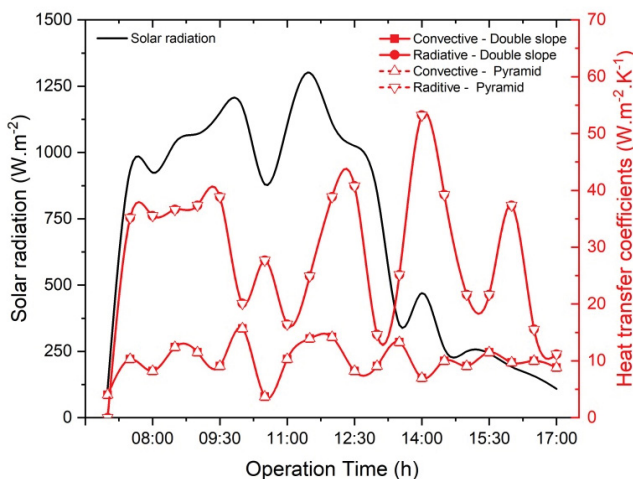
Fig. 10. External heat transfer coefficients.
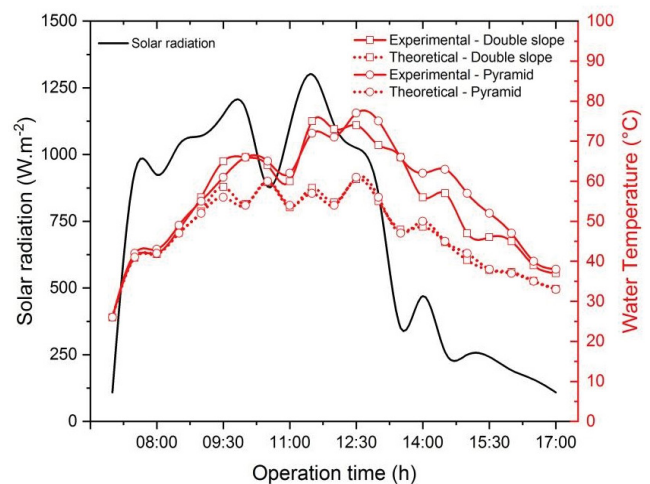
Fig. 12. Temperature profiles for the water component.

Table 4
Physico-chemical properties of waters

Physico-chemical properties	Brackish	Pyramid solar still	Double slope solar still	Unity
pH	7.0	6.10	6.15	–
Electric conductivity	11,160.0	55.14	29.88	$\mu S \cdot cm^{-1}$
Total hardness as $CaCO_3$	375.0	0.20	0.40	$mg \cdot L^{-1}$
Total alkalinity as $CaCO_3$	531.0	5.00	2.40	$mg \cdot L^{-1}$
Sodium as Na^+	1,200.0	2.00	1.00	$mg \cdot L^{-1}$
Chlorides as Cl^-	5,538.0	0.50	0.60	$mg \cdot L^{-1}$
Turbidity	4.0	3.00	3.00	NTU
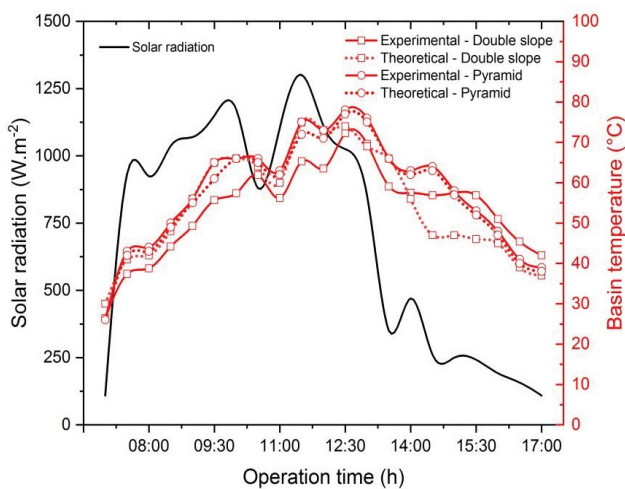
Fig. 13. Temperature profiles for the basin component.

plate temperature profiles. The Pyramid solar still has highest temperature values when compared to the double slope solar still, with maximum values of 80°C at 12:30 pm and 75°C at 12:30 pm for the two solar still, respectively.

8. Physico-chemical properties of waters

The physico-chemical properties of brackish water and desalinated water on 11/26/2021 are shown in Table 4. According to physical–chemical parameters, it was found that treatment of brackish water by the solar desalination process was effective, since the electrical conductivity, alkalinity, chlorides, total hardness, turbidity, pH and sodium were significantly reduced after desalination. The electrical conductivity is related to the number of salts dissolved in the water. The value found was 11,160.0 $\mu S \cdot cm^{-1}$ reaching 55.14 and 29.99 $\mu S \cdot cm^{-1}$, for the pyramid still and double slope still, respectively. In general, the chlorides found in groundwater come from dissolution of minerals. The reduction of this parameter was quite satisfactory, changing from 5,538.0 to 0.6 and 0.5 $mg \cdot Cl^- \cdot L^{-1}$ after the desalination process for the pyramid still and double slope still, respectively. Another significant parameter for the degree of salinity of the water is sodium, from 1,200.0 $mg \cdot Na^+ \cdot L^{-1}$ to raw water, to 2.0 and 1.0 $mg \cdot Na^+ \cdot L^{-1}$. Thus, in view of the results obtained, the shape of the stills does not affect the quality of desalinated water.

9. Conclusions

This research presents results of a comparative analysis between two passive stills with the same area of Sun exposure, but different formats, in order to verify if this characteristic influences the temperature profiles and the productivity of desalinated water. The temperature profiles of the two stills follow the incidence of solar radiation in a proportional matter. The instantaneous production of water has a distribution that follows the climatic conditions at the time of measurement and is proportional the intensity of solar radiation. The pyramid solar still produced an average of 2,508.0 $mL \cdot m^{-2}$ and the double slope solar still of 2,329.0 $mL \cdot m^{-2}$, which indicates a slightly higher yield of the pyramid still with an average of 7.13% for the experiments performed. This higher productivity can be attributed to the fact that it receives extra solar rays because it has four sides, which allow more solar radiation to be trapped inside the still throughout the day. In this way, the efficiency of solar desalinators was proven to obtain fresh water, and can be applied not only for research purposes, but also as an alternative to acquire quality water for isolated communities in the semiarid region of northeast Brazil, where there is a large number of shortage of drinking water. As future prospects, studies will be carried out coupling accessories to the system and adding materials that store energy to optimize the productivity of desalination units.

References

[1] M. Shatat, S. Omer, M. Gillott, S. Riffat, Theoretical simulation of small scale psychometric solar water desalination system in semi-arid region, Appl. Therm. Eng., 59 (2013) 232–242.
[2] R.G. Cavalcante Jr., M.A.V. Freitas, N.F. da Silva, F.R. de Azevedo Filho, Sustainable groundwater exploitation aiming at the reduction of water vulnerability in the Brazilian semi-arid region, Energies, 12 (2019) 904, doi: 10.3390/en12050904.
[3] V.P.R. Silva, F.A.S. Sousa, E.P. Cavalcanti, E.P. Souza, B.B. Silva, Teleconnections between sea-surface temperature anomalies

and air temperature in northeast Brazil, J. Atmos. Sol. Terr. Phys., 68 (2006) 781–792.

[4] L.G.M. Pessoa, M.B.G.S. Freire, J.C.A. Filho, P.R. Santos, M.F.A. Miranda, F.J. Freire, Characterization and classification of halomorphic soils in the semiarid region of northeastern Brazil, J. Agric. Sci., 11 (2019) 405–418.

[5] A.A. El-Sebaii, E. El-Bialy, Advanced designs of solar desalination systems: a review, Renewable Sustainable Energy Rev., 49 (2015) 1198–1212.

[6] M.S.S. Abujazar, S. Fatihah, A.R. Rakmi, M.Z. Shahrom, The effects of design parameters on productivity performance of a solar still for seawater desalination: a review, Desalination, 385 (2016) 178–193.

[7] C. Chen, Y. Kuang, L. Hu, Review challenges and opportunities for solar evaporation, Joule, 3 (2019) 683–718.

[8] Z.M. Omara, A.E. Kabeel, A.S. Abdullah, A review of solar still performance with reflectors, Renewable Sustainable Energy Rev., 68 (2017) 638–649.

[9] M.S. Sodha, R.S. Adhikari, A. Kumar, Techno-economic model of a solar still coupled with a solar flat-plate collector, Int. J. Energy Res., 14 (1990) 533–552.

[10] S. Kumar, G.N. Tiwari, Estimation of internal heat transfer coefficients of a hybrid (PV/T) active solar still, Sol. Energy, 83 (2009) 1656–1667.

[11] G.N. Tiwari, A. Kumar, Nocturnal water production by tubular solar stills using waste heat to preheat brine, Desalination, 69 (1988) 309–318.

[12] S.K. Singh, V.P. Bhatnagar, G.N. Tiwari, Design parameters for concentrator assisted solar distillation system, Energy Convers. Manage., 37 (1996) 247–252.

[13] H.Ş. Aybar, Mathematical modeling of an inclined solar water distillation system, Desalination, 190 (2006) 63–70.

[14] K.H. Nayi, K.V. Modi, Pyramid solar still: a comprehensive review, Renewable Sustainable Energy Rev., 81 (2018) 136–148.

[15] R.V. Dunkle, Solar Water Distillation: The Roof Type Still and a Multiple Effect Diffusion Still, International Developments in Heat Transfer, ASME, Proc. International Heat Transfer, Part V, University of Colorado, Melbourne, CSIRO, 1961, pp. 895–902.

[16] O.O. Badran, Experimental study of the enhancement parameters on a single slope solar still productivity, Desalination, 209 (2007) 136–143.

[17] Y.A.F. El-Samadony, W.M. El-Maghlany, A.E. Kabeel, Influence of glass cover inclination angle on radiation heat transfer rate within stepped solar still, Desalination, 384 (2016) 68–77.

[18] E. Rubio, J.L. Fernández, M.A. Porta-Gándara, Modeling thermal asymmetries in double slope solar stills, Renewable Energy, 29 (2004) 895–906.

[19] T. Abderachid, K. Abdenacer, Effect of orientation on the performance of a symmetric solar still with a double effect solar still (comparison study), Desalination, 329 (2013) 68–77.

[20] P. Malaiyappan, N. Elumalai, Asymmetrical solar still coupled with the mini solar pond: performance evaluation on clear, partially cloudy and cloudy days, Appl. Mech. Mater., 787 (2015) 22–26.

[21] N.H.A. Rahim, New method to store heat energy in horizontal solar desalination still, Renewable Energy, 28 (2003) 419–433.

[22] S.B. Sadineni, R. Hurt, C.K. Halford, R.F. Boehm, Theory and experimental investigation of a weir-type inclined solar still, Energy, 33 (2008) 71–80.

[23] M. Sakthivel, S. Shanmugasundaram, T. Alwarsamy, An experimental study on a regenerative solar still with energy storage medium – Jute cloth, Desalination, 264 (2010) 24–31.

[24] M. Boukar, A. Harmim, Parametric study of a vertical solar still under desert climatic conditions, Desalination, 168 (2004) 21–28.

[25] B.I. Ismail, Design and performance of a transportable hemispherical solar still, Renewable Energy, 34 (2009) 145–150.

[26] V. Velmurugan, K. Srithar, Performance analysis of solar stills based on various factors affecting the productivity – a review, Renewable Sustainable Energy Rev., 15 (2011) 1294–1304.

[27] S.W. Sharshir, N. Yang, G. Peng, A.E. Kabeel, Factors affecting solar stills productivity and improvement techniques: a detailed review, Appl. Therm. Eng., 100 (2016) 267–284.

[28] A.F. Muftah, M.A. Alghoul, A. Fudholi, M.M. Abdul-Majeed, K. Sopian, Factors affecting basin type solar still productivity: a detailed review, Renewable Sustainable Energy Rev., 32 (2014) 430–447.

[29] M.K. Phadatare, S.K. Verma, Influence of water depth on internal heat and mass transfer in a plastic solar still, Desalination, 217 (2007) 267–275.

[30] A.K. Tiwari, G.N. Tiwari, Effect of water depths on heat and mass transfer in a passive solar still: in summer climatic condition, Desalination, 195 (2006) 78–94.

[31] A. Ahsan, M. Imteaz, U.A. Thomas, M. Azmi, A. Rahman, N.N. Nik Daud, Parameters affecting the performance of a low cost solar still, Appl. Energy, 114 (2014) 924–930.

[32] M. Faegh, M.B. Shafii, Experimental investigation of a solar still equipped with an external heat storage system using phase change materials and heat pipes, Desalination, 409 (2017) 128–135.

[33] A.E. Kabeel, M.A. Teamah, M. Abdelgaied, G.B.A. Aziz, Modified pyramid solar still with v-corrugated absorber plate and PCM as a thermal storage medium, J. Cleaner Prod., 161 (2017) 881–887.

[34] J. Madiouli, A. Lashin, I. Shigidi, I.A. Badruddin, A. Kessentini, Experimental study and evaluation of single slope solar still combined with flat plate collector, parabolic trough and packed bed, Sol. Energy, 196 (2020) 358–366.

[35] P. Dumka, Y. Kushwah, A. Sharma, D.R. Mishra, Comparative analysis and experimental evaluation of single slope solar still augmented with permanent magnets and conventional solar still, Desalination, 459 (2019) 34–45.

[36] S. Rashidi, S. Akar, M. Bovand, R. Ellahi, Volume of fluid model to simulate the nanofluid flow and entropy generation in a single slope solar still, Renewable Energy, 115 (2018) 400–410.

[37] S.J.P. Gnanaraj, V. Velmurugan, An experimental study on the efficacy of modifications in enhancing the performance of single basin double slope solar still, Desalination, 467 (2019) 12–28.

[38] Y.A. Al-Molhem, M.A. Eltawil, Enhancing the double-slope solar still performance using simple solar collector and floatable black wicks, Environ. Sci. Pollut. Res., 27 (2020) 35078–35098.

[39] H. Yousefi, M. Aramesh, B. Shabani, Design parameters of a double-slope solar still: modelling, sensitivity analysis, and optimization, Energies, 14 (2021) 480–503.

[40] A.E. Kabeel, R. Sathyamurthy, S.W. Sharshir, A. Muthumanokar, H. Panchal, N. Prakash, C. Prasad, S. Nandakumar, M.S. El Kady, Effect of water depth on a novel absorber plate of pyramid solar still coated with TiO_2 nano black paint, J. Cleaner Prod., 213 (2019) 185–191.

[41] A. El-Sebaii, A.E. Khallaf, Mathematical modeling and experimental validation for square pyramid solar still, Environ. Sci. Pollut. Res., 27 (2020) 32283–32295.

[42] A.M. Manokar, D.P. Winston, R. Sathyamurthy, A.E. Kabeel, A.R. Prasath, Experimental investigation on pyramid solar still in passive and active mode, Heat Mass Transfer, 55 (2019) 1045–1058.

[43] D.B. Singh, I.M. Al-Helal, Energy metrics analysis of N identical evacuated tubular collectors integrated double slope solar still, Desalination, 432 (2018) 10–22.

[44] M. Fathy, H. Hassan, M.S. Ahmed, Experimental study on the effect of coupling parabolic trough collector with double slope solar still on its performance, Sol. Energy, 163 (2018) 54–61.

[45] K.V. Modi, K.H. Nayi, Efficacy of forced condensation and forced evaporation with thermal energy storage material on square pyramid solar still, Renewable Energy, 153 (2020) 1307–1319.

[46] W.H. Alawee, S.A. Mohammed, H.A. Dhahad, A.S. Abdullah, Z.M. Omara, F.A. Essa, Improving the performance of pyramid solar still using rotating four cylinders and three electric heaters, Process Saf. Environ. Prot., 148 (2021) 950–958.

[47] S.W. Sharshir, M.A. Omara, G. Elsisi, A. Joseph, A.W. Kandeal, A. Ali, G. Bedair, Thermo-economic performance improvement of hemispherical solar still using wick material with V-corrugated basin and two different energy storage materials, Sol. Energy, 249 (2023) 336–352.

[48] S.W. Sharshir, M.A. Rozza, M. Elsharkawy, M.M. Youns, F. Abou-Taleb, A.E. Kabeel, Performance evaluation of a modified pyramid solar still employing wick, reflectors, glass cooling and TiO$_2$ nanomaterial, Desalination, 539 (2022) 115939, doi: 10.1016/j.desal.2022.115939.

[49] M.E.H. Attia, A.E. Kabeel, M.E. Zayed, M. Abdelgaied, S.W. Sharshir, A.S. Abdulla, Experimental study of a hemi-spherical solar distillation system with and without rock salt balls as low-cost sensible storage: performance optimization and comparative analysis, Sol. Energy, 247 (2022) 373–384.

[50] A.E. Kabeel, M. Abdelgaied, A.R.A. Elbar, G.B. Abdelaziz, S.W. Sharshir, A.S. Abdullah, N.M. Ghazaly, M.I. Amro, A thermo-economic study of tubular solar distillers with V-corrugated basin and reflective mirrors, Sol. Energy, 247 (2022) 270–285.

[51] S.W. Sharshir, M.A. Rozza, A. Joseph, A.W. Kandeal, A.A. Tareemi, F. Abou-Taleb, A.E. Kabeel, A new trapezoidal pyramid solar still design with multi thermal enhancers, Appl. Therm. Eng., 213 (2022) 118699, doi: 10.1016/j.applthermaleng.2022.118699.

[52] H. Liu, D. Ji, M. An, A.W. Kandeal, A.K. Thakur, M.R. Elkadeem, A.M. Algazzar, G.B. Abdelaziz, S.W. Sharshir, Performance enhancement of solar desalination using evacuated tubes, ultrasonic atomizers, and cobalt oxide nanofluid integrated with cover cooling, Process Saf. Environ. Prot., 171 (2023) 98–108.

[53] S.W. Sharshir, A.W. Kandeal, A.M. Algazzar, A. Eldesoukey, M.O.A. El-Samadony, A.A. Hussien, 4-E analysis of pyramid solar still augmented with external condenser, evacuated tubes, nanofluid and ultrasonic foggers: a comprehensive study, Process Saf. Environ. Prot., 164 (2022) 408–417.

[54] A.W. Kandeal, Z. Xu, G. Peng, M.H. Hamed, A.E. Kabeel, N. Yang, S.W. Sharshir, Thermo-economic performance enhancement of a solar desalination unit using external condenser, nanofluid, and ultrasonic foggers, Sustainable Energy Technol. Assess., 52 (2022) 102348, doi: 10.1016/j.seta.2022.102348.

[55] W.S.A. Shanaba, A.H. Elsheikh, E.I. Ghandourah, E.B. Moustafa, S.W. Sharshir, Performance improvement of solar distiller using hang wick, reflectors and phase change materials enriched with nano-additives, Case Stud. Therm. Eng., 31 (2022) 101856, doi: 10.1016/j.csite.2022.101856.

[56] S.W. Sharshir, A. Joseph, A.W. Kandeal, A.A. Hussien, Performance improvement of tubular solar still using nano-coated hanging wick thin film, ultrasonic atomizers, and cover cooling, Sustainable Energy Technol. Assess., 52 (2022) 102127, doi: 10.1016/j.seta.2022.102127.

[57] M.K.B. Cardoso, K.S. Silva, C.B. Silva, G.G.C. Lima, K.M. Medeiros, C.A.P. Lima, Low-cost solar still with corrugated absorber basin for water desalination, J. Braz. Soc. Mech. Sci. Eng., 44 (2022) 214, doi: 10.1007/s40430-022-03520-z.

[58] M. Meybeck, E. Kuusisto, A. Mäkelä, E. Mälkki, Water Quality Monitoring – A Practical Guide to the Design and Implementation of Freshwater Quality Studies and Monitoring Programmes, Chapter 2 – Water Quality, Published on Behalf of United Nations Environment Programme and the World Health Organization, 1996 UNEP/WHO.

[59] C. Elango, N. Gunasekaran, K. Sampathkumar, Thermal models of solar still – a comprehensive review, Renewable Sustainable Energy Rev., 47 (2015) 856–911.

[60] S. Aggarwal, G.N. Tiwari, Convective mass transfer in a double-condensing chamber and a conventional solar still, Desalination, 115 (1998) 181–188.

[61] M. Abu-Arabi, Y. Zurigat, H. Al-Hinai, S. Al-Hiddabi, Modeling and performance analysis of a solar desalination unit with double-glass cover cooling, Desalination, 143 (2002) 173–182.

[62] Y.H. Zurigat, M.K. Abu-Arabi, Modelling and performance analysis of a regenerative solar desalination unit, Appl. Therm. Eng., 24 (2004) 1061–1072.

[63] H. Al-Hinai, M.S. Al-Nassri, B.A. Jubran, Parametric investigation of a double-effect solar still in comparison with a single-effect solar still, Desalination, 150 (2002) 75–83.

[64] Madhuri, G.N. Tiwari, Performance of solar still with intermittent flow of waste hot water in the basin, Desalination, 52 (1985) 345–357.

[65] C. Rabadia, Factors influencing the productivity of solar still, Int. J. Res. Appl. Sci. Eng. Technol., 3 (2015) 313–322.

[66] S.A. Kumar, P.S.M. Kumar, R. Sathyamurthy, A.M. Manokar, Experimental investigation on pyramid solar still with single and double collector cover-comparative study, Heat Transfer Asian Res., 49 (2020) 103–119.

[67] Y.A. Al-Molhem, M.A. Eltawil, Enhancing the double-slope solar still performance using simple solar collector and floatable black wicks, Environ. Sci. Pollut. Res., 27 (2020) 35078–35098.

[68] A. Awasthi, K. Kumari, H. Panchal, R. Sathyamurthy, Passive solar still: recent advancements in design and related performance, Environ. Technol. Rev., 7 (2018) 235–261.

[69] A. Khechekhouche, B.B. Haoua, A.E. Kabeel, M.E.H. Attia, W.M. El-Maghlany, Improvement of solar distiller productivity by a black metallic plate of zinc as a thermal storage material, J. Test. Eval., 27 (2020) 18–56.

[70] H. Al-Hinai, M.S. Al-Nassri, B.A. Jubran, Effect of climatic, design and operational parameters on the yield of a simple solar still, Energy Convers. Manage., 43 (2002) 1639–1650.

[71] H. Aburideh, A. Deliou, B. Abbad, F. Alaoui, D. Tassalit, Z. Tigrine, An experimental study of a solar still: application on the sea water desalination of Fouka, Procedia Eng., 33 (2012) 475–484.

[72] S.J.P. Gnanaraj, V.V. Gnanaraj, An experimental study on the efficacy of modifications in enhancing the performance of single basin double slope solar still, Desalination, 467 (2019) 12–28

[73] H.M. Ahmed, F.S. Alshutal, G. Ibrahim, Impact of different configurations on solar still productivity, J. Adv. Sci. Eng. Res., 4 (2014) 118–126.

[74] K. Rabhi, R. Nciri, F. Nasri, C. Ali, H.B. Bacha, Experimental performance analysis of a modified single-basin single-slope solar still with pin fins absorber and condenser, Desalination, 416 (2017) 86–93.

[75] S.A. El-Agouz, Experimental investigation of stepped solar still with continuous water circulation, Energy Convers. Manage., 86 (2014) 186–193.

[76] H.T. El-Dessouky, H.M. Ettouney, Fundamentals of Saltwater Desalination, Elsevier Science BV, 2002.

[77] N. Rahbar, A. Gharaiian, S. Rashidia, Exergy and economic analysis for a double slope solar still equipped by thermo-electric heating modules – an experimental investigation, Desalination, 420 (2017) 106–113.

[78] M.S.S. Abujazar, S. Fatihah, E.R. Lotfy, A.E. Kabeel, S. Sharil, Performance evaluation of inclined copper-stepped solar still in a wet tropical climate, Desalination, 425 (2018) 94–103.

[79] A.O. Al-Sulttani, A. Ahsan, A. Rahman, N.N. Nik Daud, S. Idrus, Heat transfer coefficients and yield analysis of a double-slope solar still hybrid with rubber scrapers: an experimental and theoretical study, Desalination, 407 (2017) 61–74.

[80] N. Setoodeh, R. Rahimi, A. Ameri, Modeling and determination of heat transfer coefficient in a basin solar still using CFD, Desalination, 268 (2011) 103–110.